Optoelectronic Investigation for High Performance 1.4 μm Pixel CMOS Image Sensors

Seong-Ho Cho, Yunki Lee, YuYeon Yu, Gibum Kim, Hongki Kim, Hyunpil Noh, Kangbok Lee, Chang-Rok, Moon, Kwangok Koh, Keehyun Paik*, and Duckhyung Lee

Advanced Technology Research Team, *Computer Aided Engineering, Memory Division, Samsung Electronics Co., Ltd., San #24 Nongseo-Dong, Giheung-Gu, Yongin-City, Gyeonggi-Do, 449-711, KOREA

TEL: +82-31-209-8676, FAX: +82-31-209-3274, e-mail: seongho1.cho@samsung.com

Abstract

We have carefully investigated optoelectronic limitations in pixel shrinkage and successfully integrated 1.4 μm pitch pixel sensors into 8M density CMOS image sensors. In order to overcome these obstacles and so improve device performance with respect to key properties, we have focused on salient design of photon guiding optics and electron collection engineering. We have optimized these sensors to increase the luminance signal of which property determines spectral response of the pixel and image quality.

Introduction

As pixel size shrinks, both the optics related to finite aperture diffraction loss of photons and the electronics to collection of photo-electrons become more important than previous generations. Recently, we have developed the smallest pixel of 1.4 μm and improved its performance based on structural optimization by numerically solving these optoelectronic problems [1]. A key to this work is to employ the narrow local interconnect and tight design rule of metal lines. Thus, we are able to effectively guide on-axis and off-axis light beams through clear metal apertures and reduce optical stack height.

A raw image taken with this pixel sensor is processed throughout different steps of signal processing such as interpolation, auto-white balance, color processing, luminance-coefficient, and Gamma correction [2]. Mostly, we focus on obtaining a high Y-SNR that is defined by luminance signal to noise ratio, measured from a processed image of the Macbeth chart after the signal processing described above. The calculation of the Y-SNR includes the overall characteristics of spectral response, crosstalk, and noise. We improve image quality by maximizing the Y-SNR, instead of fragmentary refinements of pixel characteristics. It is noteworthy that the optimized spectral shape as well as low crosstalk is more important than merely high sensitivity, in order to increase the Y-SNR.

Numerical Simulations and Measurements

Inherently, one of main caveats in small pixels design is finite aperture diffraction loss of photons at the backend structure through which photons focused from the micro-lens are guided. Especially, the aperture size of metal opening and the height of entire metallic layers affect photon delivery, severely changing sensitivity in the 1.4 μm pixels. Due to the limitation of beam delivery in the 1.4 μm pixels, beam shaping through the back-end should be performed. For instance, both the size of the beam waist and the shape of the beam around the metal opening determine the transmission of the impinging light.

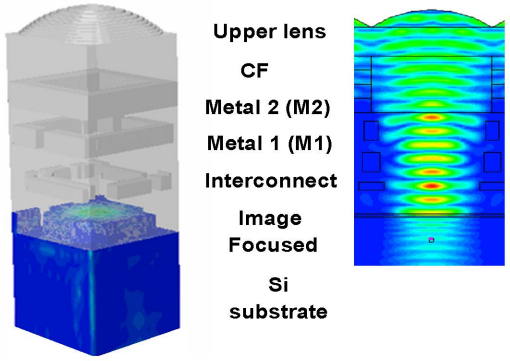

Fig.1. A three dimensional pixel of 1.4 μm pitch and a beam propagation pattern.

By calculating eq. (1) of the Fresnel diffraction through the square aperture of the pixel [3], we recognize that the propagation pattern resembles a circular aperture Fraunhoffer diffraction pattern as the image formed on the Si substrate is shown in Fig. 1,

$$\frac{jk}{2\pi z}\int_{-\infty}^{\infty}\int_{-\infty}^{\infty} square(\frac{x'}{l},\frac{y'}{l})\exp[-j\frac{k}{2z}\{(x-x')^2+(y-y')^2\}]dx'dy' \quad (1)$$

where ***square*** is an aperture function, z is a distance from the square aperture to a point in the pixel, k is a wave-vector, and l is the size of the pixel.

We conduct 2D and 3D finite-difference time-domain (FDTD) and beam propagation simulations to estimate optoelectronic photon loss throughout the backend structure and photo-electron conversion at the Si substrate. In a given curvature of the upper-lens, the opening size of the M1 critically affects the transmission of incident light in Fig. 2 as does the M2 opening. The beam loss through M2 drops more quickly than

through M1, since the beam waist is located below M2. Beam shaping is performed by optimizing lens height, equivalent to lens curvature, for efficient beam delivery in on-axis illumination in Fig. 3.

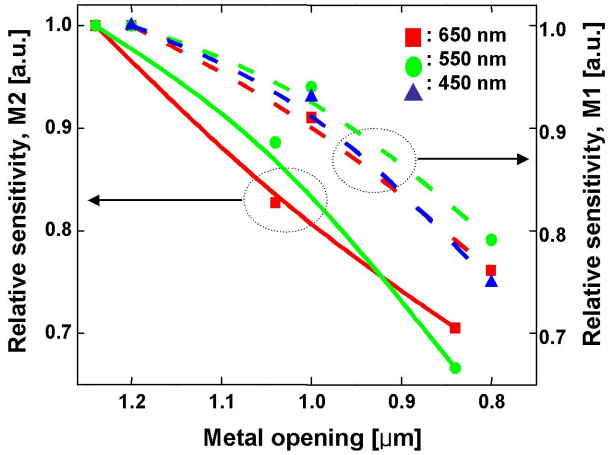

Fig.2. Sensitivity decreases as metal aperture sizes shrink in 3D FDTD simulations.

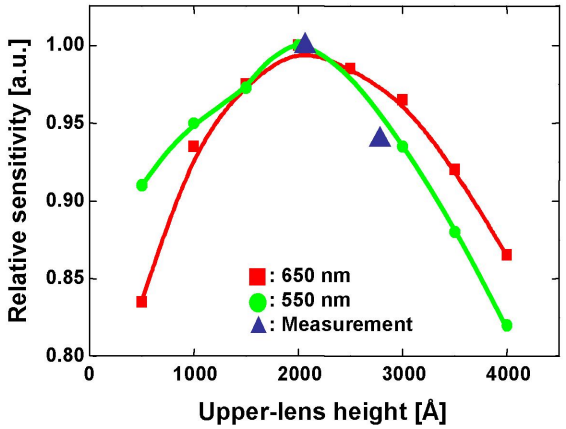

Fig.3. Sensitivity changes as lens thickness varies in 2D beam propagation method.

Fig. 4 shows the relative intensity of off-axis oblique light to three different color pixels. The measurement in Fig. 4 indicates that 3D loss is almost as twice as 2D loss, because of the assumption of infinite dimension along the other axis of the metal line. In this experiment, hand held lasers of three different colors are used. For the optimization of off-axis illumination, the lens and the color filters are shifted to the direction of light incidence.

Another crucial factor for high performance in small pixels is electrical crosstalk. Long wavelength photons deeply penetrate into the Si substrate due to low light absorption compared with other colors, diffusing and drifting to neighbor pixels. Fig. 5 elucidates how red photons move in the deep regions of the pixels. We modify the front-end structure in order to avoid electrical crosstalk between adjacent pixels for which implantation engineering strengthens photoelectron isolation. In addition, another implantation builds up a potential inclination along the flat region of the electrical potential. Thus, an effective collection of stray electrons to their own pixels is made.

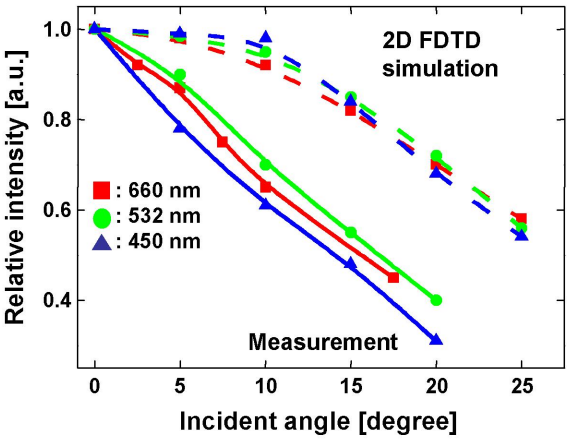

Fig.4. Sensitivity decreases as the incident angle increases.

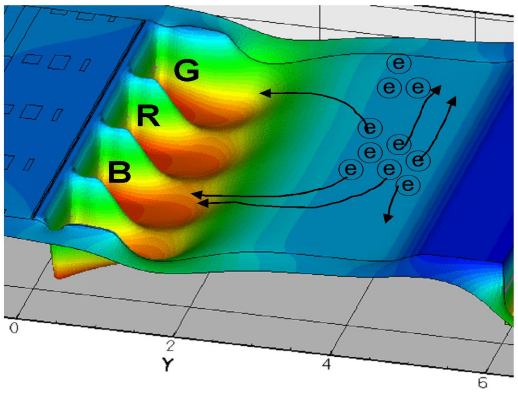

Fig.5. Electrical potential of each color pixel conceptually depicts electrons drift to adjacent pixels.

Fig. 6 shows two different spectra before and after the implantation processing for photodiode (PD) optimization. Using this method, we decrease crosstalk by 27% and increase Y-SNR by 16%, while maintaining the blooming barrier the same as before. Thus, we are confirmed that the potential wells are further stretched toward the flat region in the PD.

Fabrication and Device Performance

According to the simulation results and the design methods explained above, we successfully optimize the design and fabrication of the pixels. Mainly, W local interconnect and 65 nm CMOS design rule are employed to establish clear metal apertures in Fig. 7.

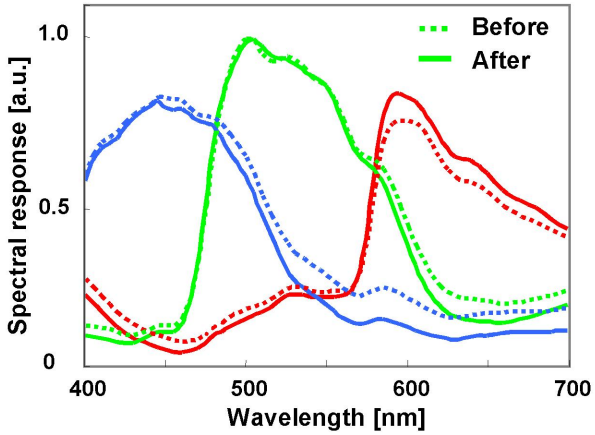

Fig.6. Relative spectral responses before and after photodiode optimization.

Additionally, the usable photodiode area is maximized using a 4-shared pixel structure of 1.75 equivalent transistors per pixel. These two techniques certainly help to maximize the fill factor and reduce optical stack height.

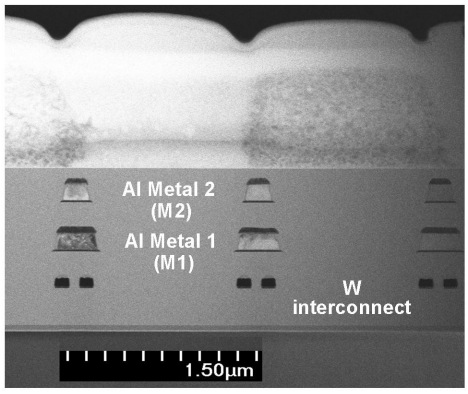

Fig.7. An image of a scanning transmission electron microscope shows a detailed vertical structure of 1.4 μm pitch pixel sensors.

The aspect ratio that is pixel height below micro-lens to pixel pitch becomes as low as 1.7, by reducing the vertical structure. Besides reduced sensitivity with 1.4μm pitch compared to larger pixel size, saturation charges tend to be diminished since the detectable PD area shrinks. As an approach to compensating degraded characteristics in pixel shrinkage, the area of the PD capacitor is especially extended with n-type doping prior to the formation of the poly-Si transfer-gate whose process flow is shown in Table 1. Thanks to this method, saturation charge is increased by 10%, and the image lag is diminished by 50%. Color filters are processed with standard negative resists, and then zero-gap upper-lenses are fabricated. Lens fill factor is approximately 90%. Important pixel parameters are enumerated in Table 2.

Table 1. Brief process flow of a conventional photodiode fabrication scheme vs a new scheme.

Structure	Conventional photodiod	Extended photodiode
	STI formation	STI formation
Key	Well and V_t implantation	Well and V_t implantation
Process	Gate-poly patterning	Photodiode formation
Flow	Photodiode formation	Gate-poly patterning
	Three Al backend steps	Two Al and one W

Table 2. Pixel parameters of 1.4 μm pitch imagers.

Item	Parameter
Number of pixels	3360 x 2476
Dynamic range	58 dB
Sensitivity	4500 e/lux·sec
Dark level @ 60°C	16 LSB/sec
Lag	< 1 LSB
Optical fill factor	60%

For a demonstration of this pixel sensor, we capture an image shown in Fig. 8.

Fig.8. A captured image of 1.4 μm 8M pixel sensors.

Conclusion

In summary, we have investigated crucial problems of low sensitivity and low saturation in 1.4 μm pixel pitch, based on advanced optoelectronic analysis and process architecture for 8M CMOS image sensors, and demonstrated their high performance.

REFERENCES

[1] Chang-Rok Moon, *et al.*, "Detailed process architecture and the characteristics of 1.4 μm pixel CMOS image sensor with 8M density," *Sym. on VLSI Circuits*, Japan, June 2007.

[2] Abbas El Gamal, *et al.*, "CMOS image sensors," *IEEE Circuits & Devices Magazine*, 2005.

[3] Max Born and Emil Wolf., *Principles of Optics*, 6th Ed., Pergamon Press, 1980.